Journal of Power Sources 246 (2014) 63–67

Contents lists available at ScienceDirect

Journal of Power Sources

journal homepage: www.elsevier.com/locate/jpowsour

Short communication

A novel dual catalyst layer structured gas diffusion electrode for enhanced performance of high temperature proton exchange membrane fuel cell

Huaneng Su, Ting-Chu Jao*, Sivakumar Pasupathi, Bernard Jan Bladergroen, Vladimir Linkov, Bruno G. Pollet

HySA Systems Competence Centre, South African Institute for Advanced Materials Chemistry, University of the Western Cape, Private Bag X17, Bellville 7535, South Africa

HIGHLIGHTS

- Novel dual CL structured GDE was prepared for high temperature PEMFC.
- Good electrode kinetics can be maintained by a PVDF outer CL.
- Reduced mass transport limitations can be realized by a proper PTFE inner CL.
- Superior performance was delivered by combining both merits of two binders.

GRAPHICAL ABSTRACT

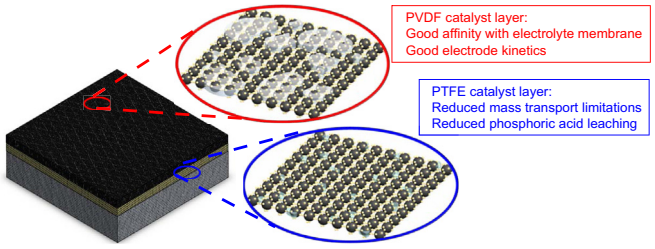

ARTICLE INFO

Article history:
Received 12 May 2013
Received in revised form
11 July 2013
Accepted 12 July 2013
Available online 26 July 2013

Keywords:
High temperature
Proton exchange membrane fuel cell
Poly(2,5-benzimidazole)
Gas diffusion electrode
Membrane electrode assembly

ABSTRACT

Gas diffusion electrode (GDE) based on a novel dual catalyst layer (CL) structure is designed to enhance the performance of poly(2,5-benzimidazole) (ABPBI)-based high temperature proton exchange membrane fuel cell (PEMFC). Differing from conventional GDE with simplex binder CL, the dual CL GDE is prepared using two different binders, in which a polyvinylidene difluoride (PVDF) CL works as the outer layer to obtain good electrode kinetics by intimately contacting with the electrolyte membrane, while a polytetrafluoroethylene (PTFE) CL works as the inner layer to reduce mass transport limitations. Single cell test and electrochemical analysis on both the dual CL GDE and conventional GDEs are performed to evaluate the effect of the novel CL structure on the fuel cell performance. The results show that significant reductions on both kinetics and mass transfer losses account for the enhanced performance of the novel dual CL structured GDE.

1. Introduction

Membrane electrode assembly (MEA) is the key part of proton exchange membrane fuel cell (PEMFC), which plays a major role in determining cell performance. At present, almost all MEAs for polybenzimidazole (PBI)-based high temperature PEMFC were prepared by catalyst coated gas diffusion layer (GDL) method, i.e., the MEA is the assembly of gas diffusion electrode (GDE) and acid-doped membrane. Therefore, the GDE characteristics, especially the structure of the catalyst layer (CL), have significant influence on the whole cell performance. Many studies have been devoted to improve GDE performance by optimizing CL structure [1–13], including selection of binder type [1–3], optimization of binder content [4–6], investigation of ink preparation [7], and

* Corresponding author. Tel./fax: +27 21 959 9310.
E-mail address: s968706@gmail.com (T.-C. Jao).
URL: http://www.hysasystems.org/

0378-7753/$ – see front matter © 2013 Elsevier B.V. All rights reserved.
http://dx.doi.org/10.1016/j.jpowsour.2013.07.062

introduction of porogens [8], etc. In early PBI-based PEMFC, PBI is the most commonly used binder for GDE preparation. Although PBI is a good membrane material due to its low gas permeability, addition of PBI as binder in the CL could impose mass transport limitation due to the film formed on the catalyst sites [13]. Alternative binders, such as polytetrafluoroethylene (PTFE) [13–15] and polyvinylidene difluoride (PVDF) [16–21], are recently considered good candidates for CL fabrication. Usually, the physicochemical properties of these binders are different from each other, consequently the electrodes based on these binders have their own advantages and shortcomings. For example, the GDEs prepared with PTFE binder usually have minimum mass transport limitations due to the high hydrophobicity and porous structure of the CLs, which can reduce the risk of PA flooding and increase the gases transport [1,14]. However, the PTFE binder which is inert and has no interaction with PA in the electrode results in a high kinetic overpotential [3]. In contrast, the GDEs prepared with PVDF binder give better electrode kinetics due to the good affinity with PA and electrolyte membrane, but the performance, especially at high current densities, is limited by the serious mass transport limitations due to the immersion of PA from PA-doped membrane [18].

In this work, a dual CL structured GDE for PBI-based high temperature PEMFC is designed by using two different binders (PTFE and PVDF), in which a PVDF-bonded CL works as the outer layer to obtain good electrode kinetics by intimately contacting with the electrolyte membrane, while a PTFE based CL works as the inner layer that was next to GDL to reduce mass transport limitations. It is envisaged that the new GDE will combine the merits of both binders; accordingly an enhanced performance can be delivered.

2. Experimental

2.1. Preparation of GDEs

Hispec 4000 Pt/C catalyst (40 wt.% Pt, Johnson Matthey) was used in this study. All GDEs were prepared by spraying method. To deposit the CL with PTFE binder, the catalyst ink was prepared by dispersing catalyst powder into a mixture of PTFE emulsion (60 wt.%, Electrochem Inc.) and isopropanol. For the CL with PVDF binder, the ink was prepared by using a lab-made 5 wt.% PVDF/DMAc solution and extra DMAc solvent. Before being used, these inks were ultrasonicated for at least 1 h for homogeneity.

All GDEs used in this study were prepared using a newly developed automatic catalyst spraying under irradiation (ACSUI) method [22]. The GDEs with dual CL structure were prepared by the following procedures. First, the catalyst ink containing PTFE binder was sprayed onto the microporous layer (MPL) of a commercially available GDL (H2315-CX196, Freudenberg, Germany), followed by calcining at 350 °C for 30 min in N_2 to form the inner CL. Then, the catalyst ink containing PVDF binder was sprayed onto the inner CL to form the outer layer. Last, the whole GDE were heat-treated at 165 °C oven overnight to evaporate the remaining DMAc. The binder contents in the inner and outer layers were 30 wt.% (PTFE) and 15 wt.% (PVDF), respectively. For simplicity, the dual CL structured GDE is denoted as DGDE. For comparison, conventional GDEs with single binder (PTFE or PVDF) CL were also prepared and denoted as PTFE GDE and PVDF GDE, respectively. The Pt loadings of all the GDEs in this study are 0.5 mg cm^{-2}.

2.2. Physical characterization of the GDEs

Pore size distributions of the GDEs were determined by using an Auto Pore IV 9500 Hg porometer (Micromeritics Instrument Corp., USA).

2.3. Single cell test and electrochemical characterization

The membranes used in this study are AB-PBI (poly(2,5-benzimidazole)), which were supplied by FuMA-Tech (fumapem® AM, ~50 μm). For doping with PA, the membranes were immersed in 85% acid solution for 24 h at 95 °C, which gave the membrane an acid doping level of about 3.8 molecules of H_3PO_4 per polymer repeating unit (PRU). The MEA was assembled by sandwiching the doped membrane between two 2.3 cm × 2.3 cm GDEs in a single cell fixture (BalticFuelCells GmbH, Germany) without a preceding hot-pressing step.

The cells were operated at 160 °C and 2 N mm^{-2} piston pressure in a FuelCon Evaluator C test station (FuelCon, Germany). Pure hydrogen was fed to the anode and air to the cathode respectively, with flow rates of 100 ml min^{-1} (hydrogen) and 250 ml min^{-1} (air), at ambient pressure, which are almost the minimum value allowed by our test system. Both hydrogen and air were used as dry gases, directly from the compressed bottles without external humidification. Prior to the recording of the polarization curves, the MEAs were activated by operating the unit cell at a constant voltage (0.55 V) under the cell temperature of 160 °C until a stable performance was obtained. The current–voltage polarization curves were obtained by measuring the current density with the stepwise decrement of voltage from 0.9 to 0.2 V, with an interval of 0.05 V. At each cell voltage, the current was measured after a hold time of 5 min to allow the cell approaching steady state. For better accuracy, single cell tests for each type were performed at least three times with different pairs of GDEs (cut from same batch), and then the average values (current densities) were determined. Normally, the relative standard deviations of these values were less than 4%.

Electrochemical impedance spectroscopy (EIS) and cyclic voltammetry (CV) were performed using an Autolab PGSTAT 30 Potentiostat/Galvanostat (Metrohm). EIS measurements were carried out at a cell voltage of 0.6 V with amplitude of 5 mV, and in the frequency range of 100 mHz–20 kHz. The impedance data were obtained by calculation and simulation with Autolab Nova software. Voltammetric measurements, undertaken to study the electrochemical active surface area (EASA), were conducted using dry N_2 at the cathode (working electrode) and dry H_2 at the anode (counter electrode and reference electrode) at room temperature (~27 °C). Cyclic voltammograms were recorded from 1.2 V to 0.05 V at a scan rate of 0.05 V s^{-1}.

3. Results and discussion

To reveal the structural differences among the CLs of the three GDEs, the pore sizes characterizations on these GDEs by mercury intrusion method were performed, as shown in Fig. 1. The distribution of pore sizes is an important parameter to GDEs since the reactant gases and water (liquid or vapor) transport are regulated by the specific volumes of small and large pores [23]. From Fig. 1, it can be seen that all three curves are similar except in the macropores zone (i.e. 5–100 μm), where the pore volume of the dual CL structured GDE is close to PTFE GDE, substantially increased comparing to pure PVDF GDE. This result is understandable considering PTFE remains insoluble in the catalyst ink, so big catalyst agglomerates are more likely formed, which would justify the larger macropores volume of the electrodes (PTFE GDE and DGDE) with PTFE CL. In the case of gas transport to the catalyst sites, the main contribution to gas transport will be due to Knudsen diffusion in the micropores and a molecular diffusion mechanism in the macropores [23]. Better mass transport would be expected for the electrodes with larger volume of the macropores, especially at high current densities.

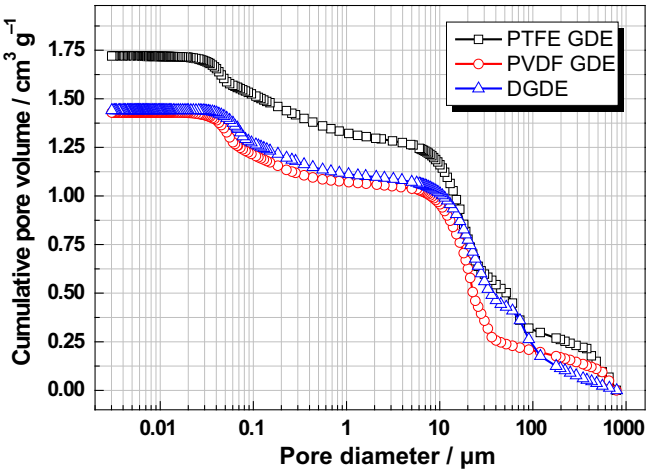

Fig. 1. Cumulative pore volume distribution of the GDEs.

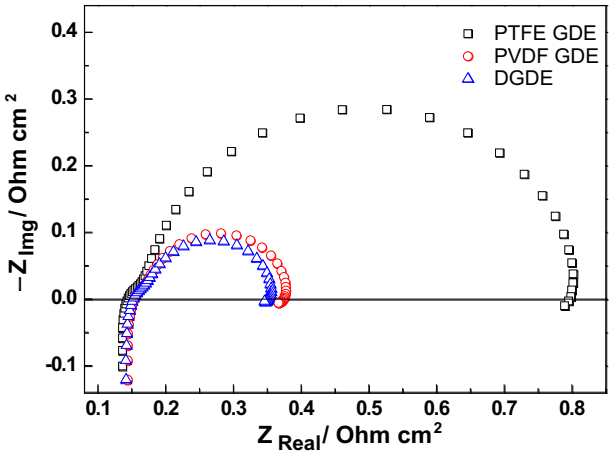

Fig. 3. *In situ* impedance curves of the MEAs with different GDEs at 0.6 V.

The performances of the single cell with the three different GDEs are shown in Fig. 2. It is clear that the conventional single CL GDEs, PTFE GDE and PVDF GDE, have their own limitations in kinetic region and mass transfer region respectively, due to the inherent properties of the used binders. In contrast, the dual CL structured GDE (DGDE) shows the advantages in the both regions; the performance at lower and medium current densities (<1 A cm^{-2}) is almost same with that for PVDF GDE, but it is obviously improved at high current densities, which explicitly indicates that DGDE kept a good electrode reaction kinetics originating from PVDF CL, and simultaneously reduced the mass transport limitations due to the proper PTFE CL. At a usual working voltage of 0.6 V, the current density is 0.424 A cm^{-2}, which is comparable to the PVDF GDE (0.42 A cm^{-2}), about twice higher than that for the PTFE GDE (0.205 A cm^{-2}). The maximum power density of the dual CL structured GDE reaches 0.535 W cm^{-2}, 13.1% and 16.1% higher than those of the PVDF and the PTFE GDEs respectively. It is worth mentioning that the maximum power density generating voltage was shifted from 0.4 V (PVDF GDE) to 0.35 V (DGDE) when the inner PTFE CL was applied, which further proves the reduction of the mass transport limitations of the dual CL structured GDE.

Fig. 3 presents the *in situ* impedance curves of the MEAs with the three GDEs at 0.6 V. Through simulation with Nova software or by taking the projection of the straight high frequency line of impedance spectrum onto the real axis [24], the corresponding ohmic resistance (R_Ω) and charge transfer resistance (R_{CT}) can be determined and summarized in Table 1. It can be seen that there is no significant difference in the ohmic resistances, which means a dual CL design did not impair the CL contact. However, the charge transfer resistance of the dual CL structured GDE is much smaller than that of the PTFE GDE, implying that the dual CL structured GDE yielded a more efficient electrochemical active layer than the latter due to the proper PVDF outer CL close to the membrane, which is further verified by the PVDF GDE that has a similar R_{CT} value.

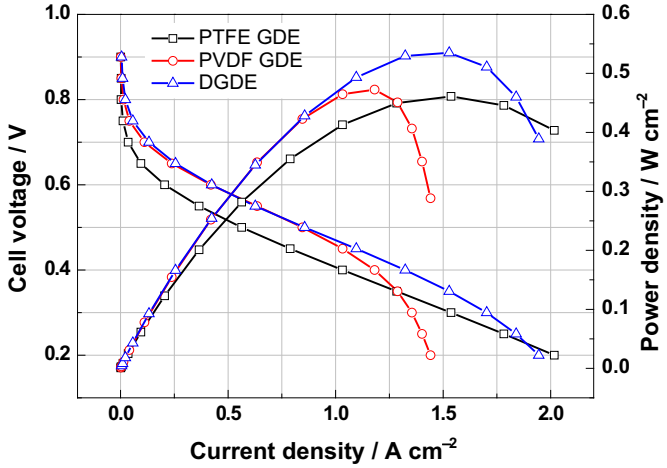

Fig. 2. Polarization curves and power density curves of the single cell with different GDEs.

To further understand how the dual CL design affects the cell performance, the *V*–*I* curves and electrochemical characteristics are theoretically analyzed to quantify the voltage loss contributions from the different electrochemical processes, i.e., activation overpotential (η_{act}), ohmic overpotential (η_{ohm}) and mass transfer overpotential (η_{mass}). Generally, both kinetic and mass transfer losses of the anode (H_2) can be neglected. Therefore, the cell voltage, E_{cell}, of a H_2/air fuel cell can be described as [25]:

$$E_{cell} = E_{rev\left(p_{H_2}, p_{O_2}, T\right)} - \eta_{act} - \eta_{ohm} - \eta_{mass} \quad (1)$$

$$E_{rev\left(p_{H_2}, p_{O_2}, T\right)} = -\frac{\Delta H - T\Delta S}{nF} + \frac{RT}{nF}\ln\frac{p_{H_2}p_{O_2}^{0.5}}{p_{H_2O}} \quad (2)$$

$E_{rev(p_{H_2}, p_{O_2}, T)}$ is the reversible potential of H_2/O_2 fuel cell, which depends on the cell temperature and the partial pressures of the reactants, equating to 1.139 V under our operating conditions calculated from Nernst equation (Eq. (2)). The ohmic overpotential, η_{ohm}, can be easily measured from *in situ* impedance measurement. Therefore, the ohmically corrected cell voltage (i.e. $E_{iR\text{-free}}$) can be directly calculated by adding η_{ohm} to the cell voltage (E_{cell}):

$$\begin{aligned} E_{iR-free} - &= E_{cell} + \eta_{ohm} = E_{cell} + iR_\Omega \\ &= E_{rev\left(p_{H_2}, p_{O_2}, T\right)} - \eta_{act} - \eta_{mass} \end{aligned} \quad (3)$$

At low current densities (<0.1 A cm^{-2}), the mass transfer overpotential (η_{mass}) can be neglected, so the *iR*-free cell voltage ($E_{iR\text{-free}}$) is controlled solely by the voltage loss due to the oxygen reduction kinetics, i.e., by the η_{act} term in Eq. (3). It was demonstrated that the cathode overpotential term (η_{act}) for Pt-catalysts follows a Tafel equation [25], relating the *iR*-free voltage loss to the logarithm of the current density (i):

Table 1
Electrochemical properties of the GDEs.

GDEs	E_{cell} at 0.4 A cm^{-2} (mV)	Tafel slope (mV dec^{-1})	η_{act} at 0.4 A cm^{-2} (mV)	η_{ohm} at 0.4 A cm^{-2} (mV)	η_{mass} at 0.4 A cm^{-2} (mV)	R_{Ω} at 0.6 V (mΩ cm^2)	R_{CT} at 0.6 V (mΩ cm^2)	EASA (m^2 g^{-1})
PTFE GDE	0.539	134	518.2	58.4	23.4	146	648	16.2
PVDF GDE	0.603	94	436.5	60.8	38.7	152	226	28.7
DGDE	0.606	107	444.2	61.6	27.2	154	207	26.3

$$\eta_{act} = a + b\log i \quad (4)$$

where a is a constant, b is the so-called Tafel slope. Accordingly, the η_{act} term can be calculated from Eq. (4) by extrapolating the Tafel plots that were obtained with the iR corrected V–I data in the low current density region (<0.1 A cm^{-2}) [3,25]. Finally, the mass transfer overpotential (η_{mass}) can be determined directly from Eq. (1) or Eq. (3).

All these electrochemical parameters for the three GDEs are tabulated for comparison, as shown in Table 1. At 0.4 A cm^{-2}, it can be seen that the ohmic voltage losses (η_{ohm}) of the three GDEs are almost same, so the kinetic loss and the mass-transfer loss are the main reasons accounting for the performance differences. Table 1 indicates that the η_{mass} values for the GDEs are between 23.4 and 38.7 mV, even smaller than the η_{ohm} values at this current density, which could be attributed to the high stoichiometries reactants (ca. 7/7.5 for H_2/Air at 0.4 A cm^{-2}) due to the small active area ($\sim$ 5 cm^2) even at low gases flow rates. However, the results still show a considerable reduction (ca. 30%) of η_{mass} for DGDE when a proper PTFE inner CL had been applied. This reduction should be more important to enhance cell performance in high current density region where mass transfer is dominant, especially for the GDEs with large dimensions.

Anyway, the kinetic overpotential (η_{act}) is the largest overpotential in these GDEs. For the PTFE GDE, the Tafel slope reaches 134 mV dec^{-1}, which results in a kinetic loss as high as 518.2 mV. However, these values can be significantly reduced when the PVDF-bonded CLs were applied next to the membranes (Table 1). Generally, the Tafel slope and the η_{act} values provide information on the kinetics of ORR on the cathodes, which is determined by the binder properties and the structure since the catalyst used in these CLs are all same. Therefore, the proper dual CL structure design is considered as the most important reason for the improved performance of the DGDE. To verify this point, CV measurements were performed to analyze the EASAs of the three GDEs, as shown in Fig. 4. The corresponding EASAs were calculated from the H_2 desorption peak of each voltammogram and the results are also summarized in Table 1. The EASA of the dual CL structured GDE is about 26.3 m^2 g^{-1}, which is comparable with the PVDF GDE, about 62% higher than that for PTFE GDE. It demonstrates that the dual CL structure design, in which the PVDF CL acts as outer layer to contact with membrane, is reasonable because the PVDF binders can interact with PA and PA-doped membrane more easier than PTFE dose due to the good affinity, consequently abundant triple-phase boundaries can be obtained at the interface between the CL and the membrane where the electrochemical reaction mainly occurs [26,27].

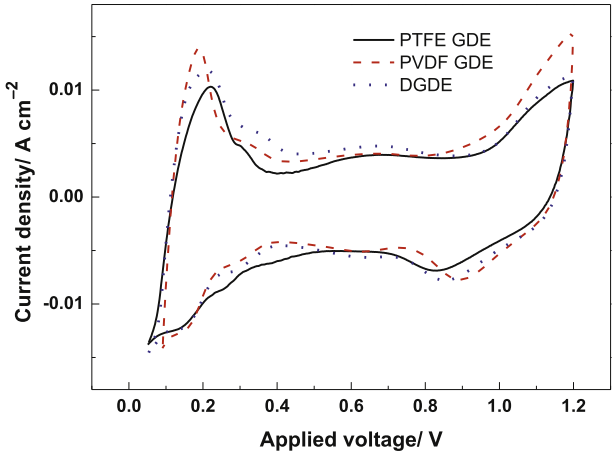

Fig. 4. Cyclic voltammograms of the MEAs with different GDEs.

4. Conclusions

GDE with a novel dual CL structure was prepared using two binders with different properties. The new GDE combines the merits of the two binders, and achieves excellent performance. Polarization test and electrochemical characterizations indicate that the performance improvement is attributable to the significant reductions on both kinetics and mass transfer losses. We conclude that good electrode kinetic and mass transport can be realized by designing a proper dual CL structure, resulting in superior performance.

Acknowledgments

This work is supported by Hydrogen and Fuel Cell Technologies RDI Programme (HySA), funded by the Department of Science and Technology in South Africa (project KP1-S01).

References

[1] P. Mazúr, J. Soukup, M. Paidar, K. Bouzek, J. Appl. Electrochem. 41 (2011) 1013–1019.
[2] A.D. Modestov, M.R. Tarasevich, V.Y. Filimonov, A.Y. Leykin, J. Electrochem. Soc. 156 (2009) B650–B656.
[3] J.O. Park, K. Kwon, M.D. Cho, S.G. Hong, T.Y. Kim, D.Y. Yoo, J. Electrochem. Soc. 158 (2011) B675–B681.
[4] J.-H. Kim, H.-J. Kim, T.-H. Lim, H.-I. Lee, J. Power Sources 170 (2007) 275–280.
[5] J. Lobato, P. Cañizares, M.A. Rodrigo, J.J. Linares, F.J. Pinar, Int. J. Hydrogen Energy 35 (2010) 1347–1355.
[6] M. Mamlouk, K. Scott, Int. J. Hydrogen Energy 35 (2010) 784–793.
[7] J. Lobato, M.A. Rodrigo, J.J. Linares, K. Scott, J. Power Sources 157 (2006) 284–292.
[8] C. Pan, Q. Li, J.O. Jensen, R. He, L.N. Cleemann, M.S. Nilsson, N.J. Bjerrum, Q. Zeng, J. Power Sources 172 (2007) 278–286.
[9] O.E. Kongstein, T. Berning, B. Børresen, F. Seland, R. Tunold, Energy 32 (2007) 418–422.
[10] J. Lobato, P. Cañizares, M.A. Rodrigo, J.J. Linares, D. Úbeda, F.J. Pinar, Fuel Cells 10 (2010) 312–319.
[11] J. Lobato, P. Canizares, M.A. Rodrigo, D. Ubeda, F.J. Pinar, J.J. Linares, Fuel Cells 10 (2010) 770–777.
[12] F. Seland, T. Berning, B. Børresen, R. Tunold, J. Power Sources 160 (2006) 27–36.
[13] M. Mamlouk, K. Scott, Int. J. Energy Res. 35 (2011) 507–519.
[14] C. Wannek, W. Lehnert, J. Mergel, J. Power Sources 192 (2009) 258–266.
[15] C. Wannek, B. Kohnen, H.F. Oetjen, H. Lippert, J. Mergel, Fuel Cells 8 (2008) 87–95.
[16] Y. Oono, A. Sounai, M. Hori, J. Power Sources 210 (2012) 366–373.
[17] Y. Oono, T. Fukuda, A. Sounai, M. Hori, J. Power Sources 195 (2010) 1007–1014.
[18] Y. Oono, A. Sounai, M. Hori, J. Power Sources 189 (2009) 943–949.
[19] Y. Zhai, H. Zhang, D. Xing, Z.-G. Shao, J. Power Sources 164 (2007) 126–133.

[20] G. Liu, H. Zhang, J. Hu, Y. Zhai, D. Xu, Z.-G. Shao, J. Power Sources 162 (2006) 547–552.
[21] Y. Zhai, H. Zhang, Y. Zhang, D. Xing, J. Power Sources 169 (2007) 259–264.
[22] H. Su, S. Pasupathi, B.J. Bladergroen, V. Linkov, B.G. Pollet, J. Power Sources 242 (2013) 510–519.
[23] H.-K. Lee, J.-H. Park, D.-Y. Kim, T.-H. Lee, J. Power Sources 131 (2004) 200–206.
[24] A.A. Kulikovsky, M. Eikerling, J. Electroanal. Chem. 691 (2013) 13–17.
[25] H.A. Gasteiger, S.S. Kocha, B. Sompalli, F.T. Wagner, Appl. Catal. B 56 (2005) 9–35.
[26] H.-N. Su, S.-J. Liao, Y.-N. Wu, J. Power Sources 195 (2010) 3477–3480.
[27] H.-N. Su, Q. Zeng, S.-J. Liao, Y.-N. Wu, Int. J. Hydrogen Energy 35 (2010) 10430–10436.